

Islanded microgrid: hybrid energy resilience optimization

Veeranjaneyulu Gopu¹, Mudakapla Shadaksharappa Nagaraj²

¹Department of Electrical and Electronics Engineering, Visvesvaraya Technological University, Belagavi, India

²Department of Electrical and Electronic Engineering, Bapuji Institute of Engineering and Technology, Davanagere, India

Article Info

Article history:

Received Jan 28, 2024

Revised Mar 27, 2024

Accepted Apr 6, 2024

Keywords:

Energy storage system

High gain DC-DC converter

Kalman filter

Power management algorithm

Sliding mode current controller

Super capacitor

ABSTRACT

To maintain a dependable and sustainable power supply in a microgrid system, it is crucial to combine renewable energy sources with hybrid energy backup. To achieve maximum output power from solar source, a high gain DC-DC boost converter is managed using the dual Kalman filter based perturb and observe approach. A sliding mode current controller at a three phase inverter with an LC filter is intended to follow an undisturbed reference voltage. To effectively manage the power flow and optimize the utilization of available resources, a robust power management algorithm is required. The novel power management algorithm for a solo operated renewable distribution generation unit with hybrid energy backup in a microgrid is introduced. The algorithm aims to dynamically allocate power among various sources, storage systems, and loads, considering their characteristics and the overall system constraints. The algorithm utilizes sliding mode control techniques to regulate the current flow from the renewable generator and effectively manage the power allocation among different energy sources, storage systems, and loads.

This is an open access article under the [CC BY-SA](https://creativecommons.org/licenses/by-sa/4.0/) license.



Corresponding Author:

Veeranjaneyulu Gopu

Department of Electrical and Electronics Engineering, Visvesvaraya Technological University

Belagavi, India

Email: gvvtu2023@gmail.com

1. INTRODUCTION

Microgrid systems, characterized by the integration of renewable energy resources and hybrid energy backup, have garnered significant attention in recent years as they offer a sustainable and reliable power supply solution [1]-[3]. Maximizing the utilization of renewable energy resources such as photovoltaic (PV) systems is crucial for enhancing the overall energy efficiency [4]. The output power from high gain DC-DC boost converters must be optimized to do this, which calls for cutting-edge control techniques like the dual Kalman filter (DKF) based perturb and observe (P&O) method [5]. Furthermore, effective power management within microgrids is essential to ensure a stable and efficient energy supply [6]. This paper introduces a novel power management algorithm designed explicitly for standalone operated renewable distribution generation unit with hybrid energy backup in microgrid systems. The primary objective of this algorithm is to dynamically allocate power among various energy sources, energy storage systems, and loads while considering their distinct characteristics and adhering to system-wide constraints [7].

Microgrids are localized energy distribution systems that may run independently of or in combination with the utility grid, providing increased sustainability and resilience [8]. The integration of renewable energy resources, such as photovoltaic systems and wind turbines, is a common feature in microgrids, contributing to reduced carbon emissions and increased reliance on clean energy [9]. To maintain a consistent and stable energy supply, advanced power management strategies are required due to the intermittent and variable nature of renewable energy sources [10]. Hybrid energy backup solutions,

combining renewable sources with conventional generators or energy storage systems, play a pivotal role in mitigating the intermittency of renewable energy generation [11]. These systems provide a reliable source of power during periods of low renewable energy production or energy demand spikes, ensuring uninterrupted power supply in microgrids [12]. The integration of such hybrid energy backup is crucial for achieving the overall sustainability and reliability goals of microgrid systems [13].

The utilization of advanced control strategies is fundamental to achieving optimal power generation and distribution in microgrids [14]. One such strategy, the DKF based P&O method, is employed to maximize the output power from high gain DC-DC boost converters connected to photovoltaic sources [15]. The total effectiveness of energy harvesting is increased because to this technique's effective tracking of the photovoltaic system's maximum power point (MPP) under a variety of operating situations.

2. THE PROPOSED METHOD

The test system supports local loads [16] and the excess power is injected into the main grid via feeders, although this is rare due to typically higher load demands. The network operates in grid-connected and islanding modes [17], where DG units synchronize with the grid and only the PV source supports critical load during islanding. Power management algorithm monitors grid parameters, disconnecting non-essential load when necessary and adjusting PV-battery-SC DG unit operations to compensate for critical load [18], [19].

The proposed system is configured with three DG units connected to four buses to compensate the local loads. Here first bus is interconnected with solar unit and with a backup source of combination supercapacitor, battery. Wind farm is tagged to bus 3 and a fuel cell interline with bus 4. Entire DG unit and a backup unit is handled by power management algorithm [20] and interconnected with the grid. The inline structure at bus 1 is shown Figure 1.

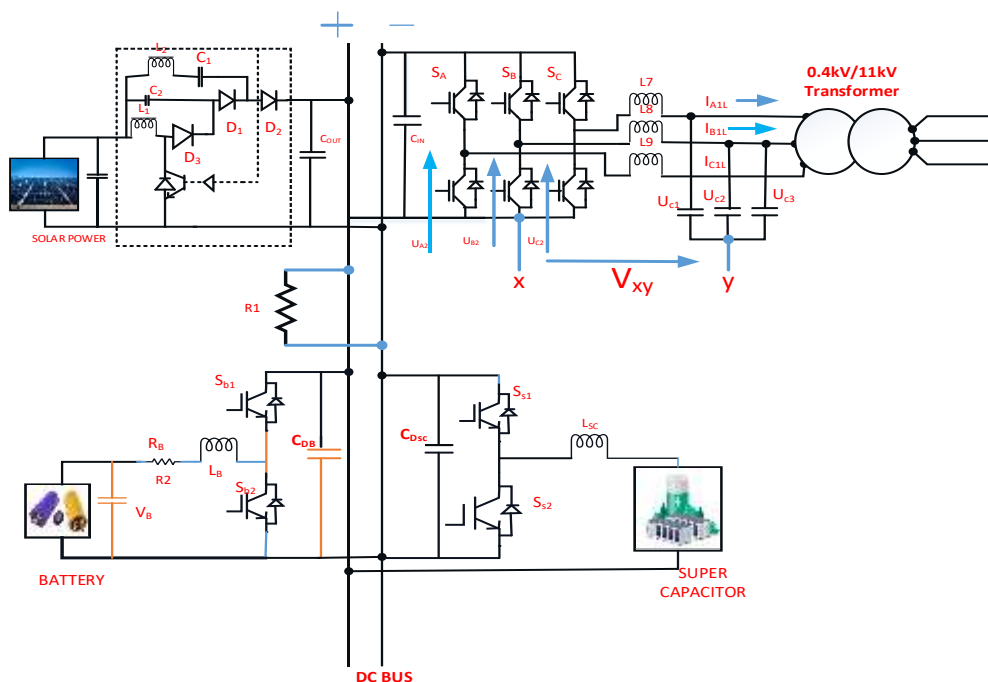


Figure 1. Sample solar module with battery and supercapacitor

In the system, a DC bus links the solar source, battery, and inverter, with a DC-DC boost converter maximizing solar power. An inverter with a sliding mode controller converts DC to AC power, ensuring grid compatibility and high-quality output. As observed from the algorithm, initially the system operates synchronously with the grid. The active and reactive power control is not implemented and $P_{pv} + P_{wind} + P_{fc} \cong P_{grid}$. The reactive power requirement of load group is adjusted by the grid itself. Here assumed that entire load is compensated by the solar source itself to know the effectiveness of islanding condition. The power management flowchart shown in Figure 2 includes the sliding mode current controller to effectively trace the reference current values.

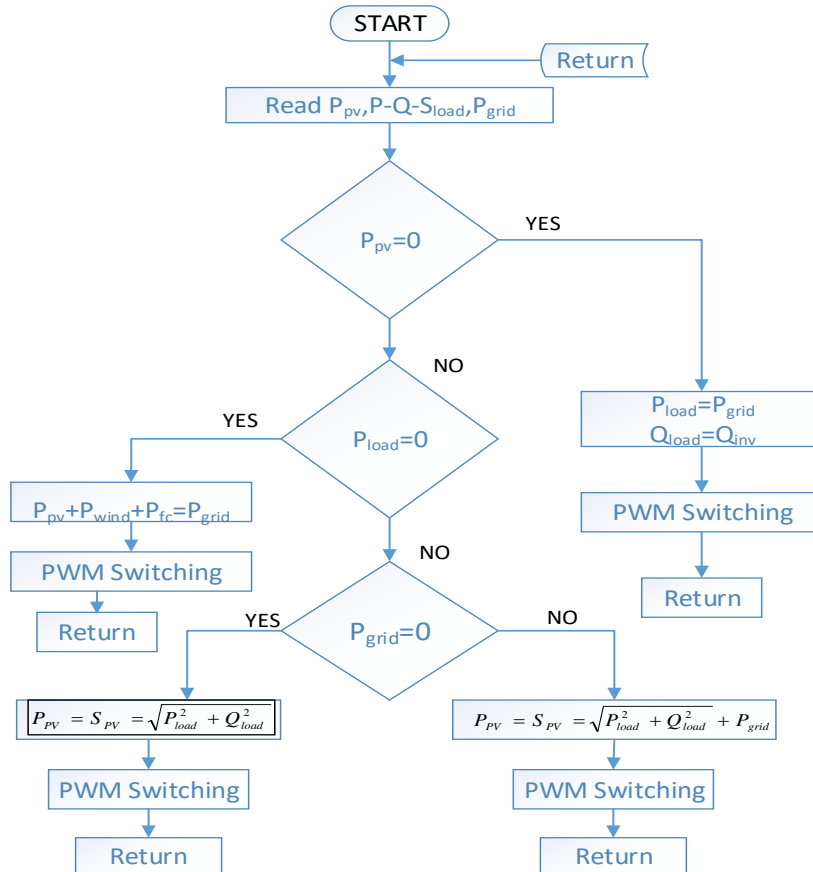


Figure 2. Power management flowchart at bus 1

2.1. Control of high gain dc-dc converter

The Kalman MPPT algorithm is a feedback control system that constantly monitors the solar panel's output voltage and current to ensure that it is operating at the most efficient point. The algorithm is named after Rudolf Kalman, who developed the Kalman filter, a mathematical algorithm used to estimate state variables from noisy measurements. The Kalman MPPT algorithm [21] is more complex than other MPPT algorithms such as the P&O algorithm, but it offers several advantages. It is more accurate at tracking the MPP and more robust to noise. Overall, the Kalman MPPT algorithm is a powerful tool for improving the efficiency of solar photovoltaic systems. It is particularly well-suited for applications where maximum power extraction is critical, such as in remote power systems and electric vehicles. The state and output are given by (1) and (2).

$$Y(x + 1) = PY(x) + QU(x) + RZ(x) \tag{1}$$

$$O(x) = EY(x) + F(x) \tag{2}$$

U(x), O(x), and Y(x) represent the input, state, and output signals respectively. Measurement noise is represented by F(x), whereas process noise is represented by Z(x). To estimate the real voltage mentioned below, time update and measurement adjustment are made.

The Kalman gain was initially calculated using (3). The calculated real voltage and error covariance have been updated in accordance with step two from (4) and (5). In (6) and (7) are time update equations. In time updating, $\hat{J}_{act}[C]$ & $M[C]$ must be used to anticipate the voltage $\hat{J}_{act}[C+1]$ and error covariance $M[C+1]$. Finally, higher than $\hat{J}_{act}[C]$, the estimated voltage $\hat{J}_{act}[C+1]$ will approach the maximum power point. The predicted voltage $\hat{J}_{act}[C+1]$ may therefore be shown to be closer to MPP than the actual value $\hat{J}_{act}[C]$. N is the plant's process noise, N is the measurement noise covariance, and B is the step size. The Kalman algorithm is used to predict the voltage of the solar panel in the next time step, based on the current

voltage and current measurements. The PI controller uses this voltage error to produce pulses for the DC/DC converter switch. The voltage error is the difference between the present voltage and the planned value. The solar panel is constantly running at its peak power level thanks to its feedback control technology.

Measurement update (correct):

$$G_{[c]} = M_{[c]} - [M_{[c]} + N]^{-1} \quad (3)$$

$$\hat{J}_{act[c]} = \hat{J}_{act[c]} + L_{[c]}[J_{ref[c]} - \hat{J}_{act[c]}] \quad (4)$$

$$M_{[c]} = [1 - J_{[c]}]M_{[c]} \quad (5)$$

Time update (predict):

$$\hat{J}_{act[c+1]} = \hat{J}_{act[c]} + B \frac{K[c] - K[c-1]}{J[c] - J[c-1]} \quad (6)$$

$$M_{[c+1]} = M_{[c]} + N \quad (7)$$

3. RESEARCH METHOD

To ensure robust and adaptable power management, a sliding mode current controller is introduced in this research [22]. Sliding mode control techniques have demonstrated their effectiveness in regulating the current flow from renewable generators, effectively managing power allocation among different energy sources, storage systems, and loads [23]. This approach is well-suited for handling transient conditions, maintaining stable power output and optimizing energy utilization within the microgrid [24].

Sliding mode control is a robust control technique that ensures accurate tracking and disturbance rejection in dynamic systems. The idea behind sliding mode control is to drive the system state onto a predefined sliding manifold, which guarantees robustness against model uncertainties and external disturbances. In the context of power management, sliding mode control [25] can be employed to regulate the current flow from the renewable generator, enabling precise control and stability in the microgrid system. U_{dc}-the DC link voltage; I_{A1L}, I_{B1L}, I_{C1L}-the currents through the filter inductors; U_{A2}, U_{B2}, U_{C2} -the voltage across the lower switches; I_{T1}, I_{T2}, I_{T3}-The currents flowing through the three phase transformer; U_{C1}, U_{C2}, U_{C3}-the Voltage across the filter capacitors.

Using the KVL, the parameters are I and U are the states of three phases A, B and C. Voltage across the switches are the controls variables and transformer currents I_{r1}, I_{r2}, I_{r3} are the measured disturbances. These all shown in (8).

$$\left. \begin{aligned} \frac{dI_{A1L}}{dt} &= \frac{1}{L}(U_{A2} + V_{xy} - U_{C1}) \\ \frac{dI_{B1L}}{dt} &= \frac{1}{L}(U_{B2} + V_{xy} - U_{C2}) \\ \frac{dI_{C1L}}{dt} &= \frac{1}{L}(U_{C2} + V_{xy} - U_{C3}) \\ \frac{dU_{C1}}{dt} &= \frac{1}{C}(I_{A1L} - I_{T1}) \\ \frac{dU_{C2}}{dt} &= \frac{1}{C}(I_{B1L} - I_{T2}) \\ \frac{dU_{C3}}{dt} &= \frac{1}{C}(I_{C1L} - I_{T3}) \end{aligned} \right\} \quad (8)$$

3.1. Sliding mode controller design

The system output phase voltages are aligned with the specified references U_{ref1}, U_{ref2} and U_{ref3} to ensure optimal performance as shown in (9). where Φ_1 , Φ_2 and Φ_3 are the angle phases set to 0°, 120° and 240° respectively. In (10) shows the designed error variables.

$$\left. \begin{aligned} U_{ref1} &= A \sin(\omega t + \phi_1) \\ U_{ref2} &= A \sin(\omega t + \phi_2) \\ U_{ref3} &= A \sin(\omega t + \phi_3) \end{aligned} \right\} \quad (9)$$

$$\left. \begin{aligned} e_1 &= U_{ref1} - U_{c1} \\ e_2 &= U_{ref2} - U_{c2} \\ e_3 &= U_{ref3} - U_{c3} \end{aligned} \right\} \tag{10}$$

The cornerstone of sliding mode control lies in the selection of an appropriate sliding surface. This surface serves as a dynamic constraint, meticulously sculpted by a trio of control variables α_1 , α_2 , and α_3 collectively orchestrate the system's trajectory. Let's go back to the error (10) and differentiate both sides of each (11).

$$\begin{aligned} \dot{e}_1 &= \dot{U}_{ref1} - \frac{1}{C} (I_{A1L} - I_{T1}) \\ \dot{e}_2 &= \dot{U}_{ref2} - \frac{1}{C} (I_{B1L} - I_{T2}) \\ \dot{e}_3 &= \dot{U}_{ref3} - \frac{1}{C} (I_{C1L} - I_{T3}) \end{aligned} \tag{11}$$

When control variables are absent in the first derivative of error functions, a second differentiation is necessary to reveal their influence. The second derivative of the error functions marks the initial emergence of control variables, signifying an error degree of 2. To construct a first-order sliding mode controller, sliding surfaces must be selected to encompass both error terms and their first time derivatives.

The functions which selected for the sliding surface are shown in (12).

$$\left. \begin{aligned} \alpha_1 &= \beta_1 e_1 + \dot{e}_1 \\ \alpha_2 &= \beta_2 e_2 + \dot{e}_2 \\ \alpha_3 &= \beta_3 e_3 + \dot{e}_3 \end{aligned} \right\} \tag{12}$$

The control law comprises two distinct components: a continuous component known as the equivalent control, and a discontinuous component. These elements are mathematically expressed in (13).

$$\left. \begin{aligned} U_{A2} &= U_{eq1} + U_{dis1} \\ U_{B2} &= U_{eq2} + U_{dis2} \\ U_{C2} &= U_{eq3} + U_{dis3} \end{aligned} \right\} \tag{13}$$

4. RESULTS AND DISCUSSION

Figure 3 shows the waveforms which explores the details regarding the contribution of power sharing from the grid, Figure 3(a) shows real and reactive power injected to grid, Figure 3(b) shows the grid voltage which is maintained by the feeder. Initially at 0 seconds both real and reactive power is injected to distribution network and at 1 sec. the grid is isolated from the distributed network even the feeder bus voltage also dribble to zero shows the islanding mode of the considered network through waveforms.

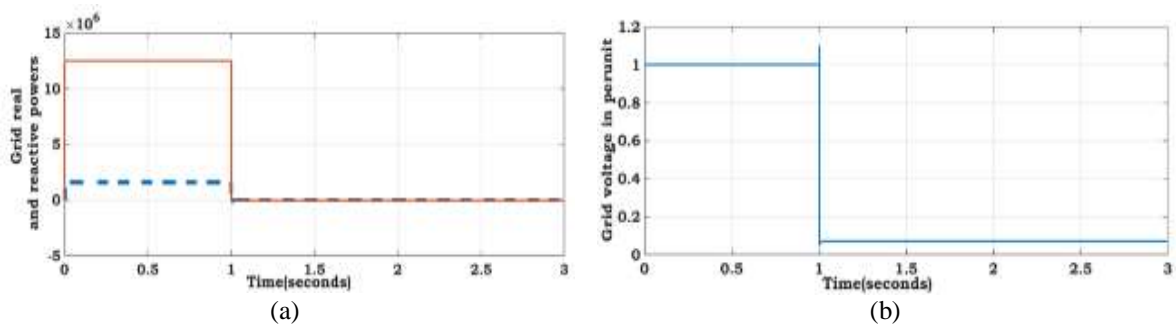


Figure 3. Grid partakers (a) P & Q injected to distribution network and (b) grid voltage in per unit

Figure 4 shows the power supplied by DG unit connected at bus 1 without backup. Figures 4(a) and (b) shows the waveforms of real and reactive powers at bus 1. Figure 5 shows the power supplied by the DG unit connected at bus 2 without backup. Figures 5(a) and (b) shows the waveforms of real and reactive powers at bus 2. Figure 6 shows the power supplied by the DG unit connected at bus 3 without backup. Figures 6(a) and (b) shows the waveforms of real and reactive powers at bus 3. The real power generated at bus 1, bus 2, bus 3 are set at 95 kW, 45 kW and 35 kW respectively. The measured values proved that the major contribution is from the DG unit connected at bus 1. Hence this paper focusing to test and contributing to eliminate the setbacks of islanding mode operation. The DG units are not able to provide any active power to the load once the grid is disconnected, even though they are still injecting reactive power. This is because the DG units are not designed to operate in islanding mode. To explore system performance during islanding events, a novel system design is proposed, seamlessly integrating a DG1 unit with backup and PMA modules. This innovative configuration empowers the DG1 unit to reliably sustain essential loads, even in the absence of the primary power source from the distribution network.

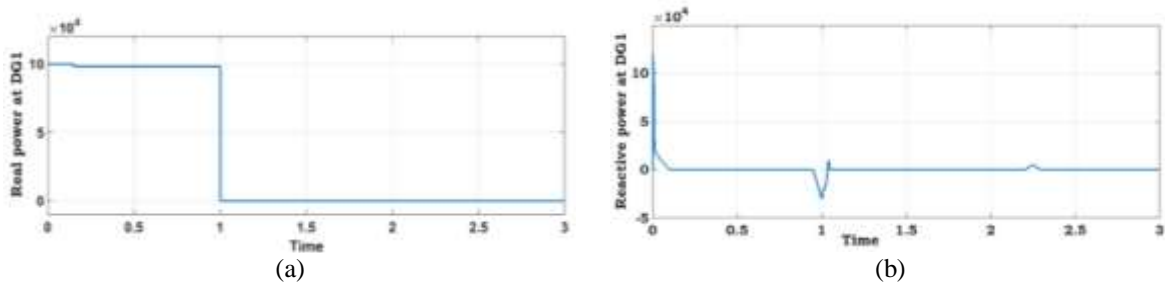


Figure 4. Power supplied by the DG unit connected at bus 1 without backup (a) real power and (b) reactive power

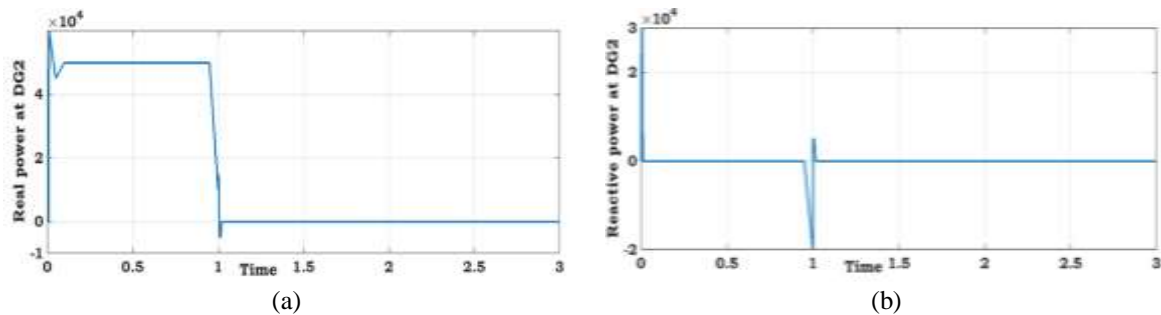


Figure 5. Power supplied by the DG unit connected at bus 2 without backup (a) real power and (b) reactive power

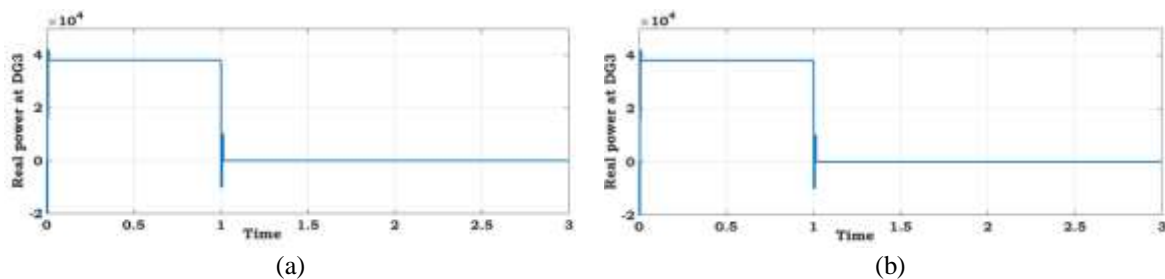


Figure 6. Power supplied by the DG unit connected at bus 3 without backup (a) real power and (b) reactive power

Figure 7 shows the power supplied by the DG unit connected at bus 1 with backup, Figures 7(a) and (b) shows real and reactive power waveforms at bus 1. Figure 8 shows the power supplied by the DG unit connected at bus 2 with backup, Figures 8(a) and (b) shows real and reactive power waveforms at bus 2. Figure 9 shows the power supplied by the DG unit connected at bus 3 with backup, Figures 9(a) and (b) shows real and reactive power waveforms at bus 3.

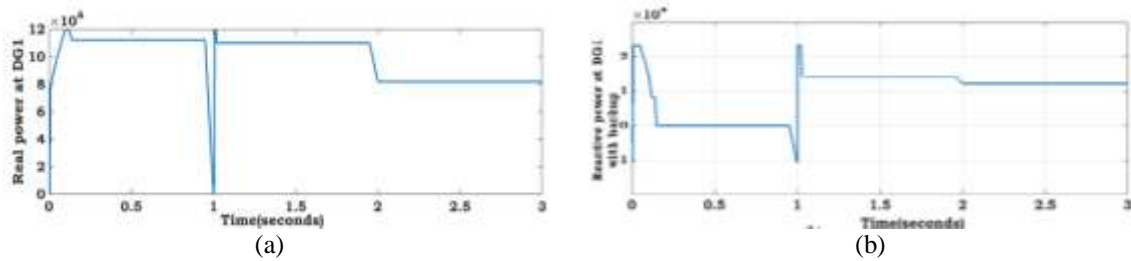


Figure 7. Power supplied by DG unit connected at bus 1 with backup (a) real power and (b) reactive power

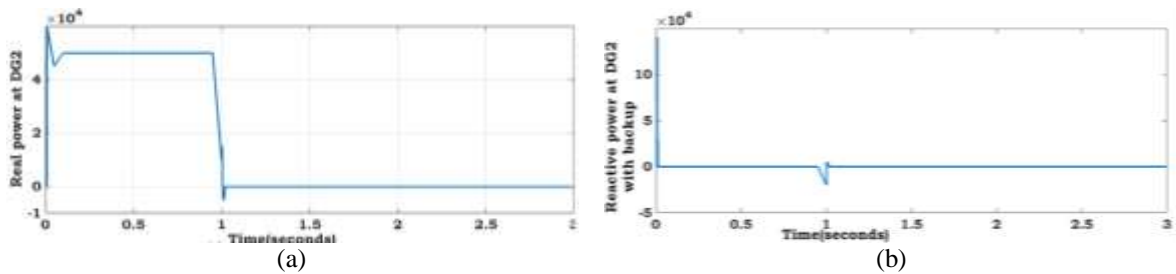


Figure 8. Power supplied by DG unit connected at bus 2 with backup (a) real power and (b) reactive power

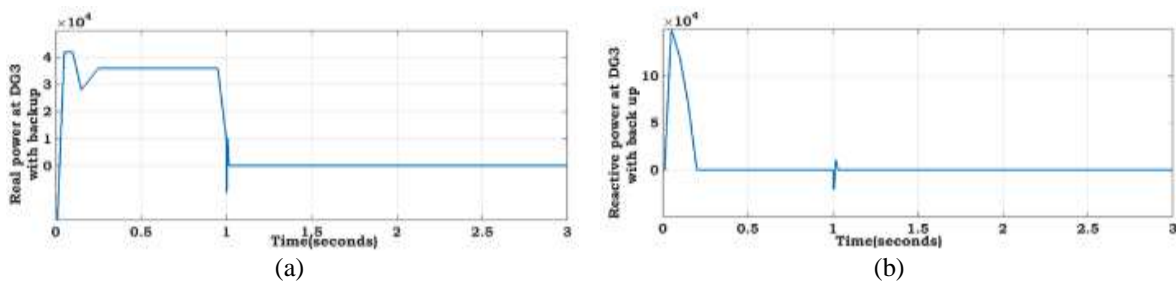


Figure 9. Power supplied by DG unit connected at bus 3 with backup (a) real power and (b) reactive power

Upon grid disconnection at 1 second, the DG1 unit gracefully steps in to maintain power continuity, supplying a robust 110 kW of active power to the load. However, when irradiation levels dip to 500 W/m² at 2 seconds, DG1's power output experiences a decline to 80 kW. In stark contrast, DG2 and DG3 units falter instantaneously due to their lack of backup or PMA modules, highlighting their vulnerability in such scenarios. Figure 10 provide a detailed graphical exploration of the power output generated by each module within the DG1 unit, offering valuable insights into their collective performance.

Figure 10 shows the power output of the different modules in the DG1 unit, including the PV panels, battery, and supercapacitor (SC). Initially, the battery and SC are providing 4 kW and 15 kW of power, respectively. Figure 11 shows the real and reactive power consumption of essential and non-essential loads. With the grid disconnected, Load critical needs are met through a coordinated surge of power from the battery and supercapacitor, demonstrating the system's ability to prioritize essential functions. Acting with surgical precision, the power management algorithm swiftly severs the non-essential load from the network, ensuring that the microgrid's precious energy reserves flow solely to the critical load.

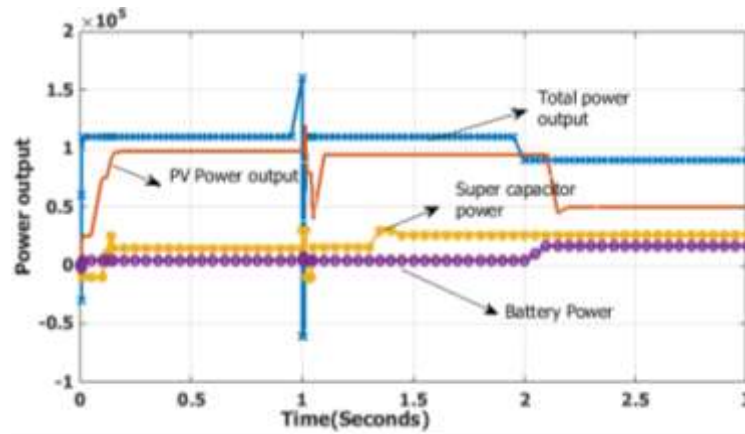


Figure 10. Output power of all modules at bus 1

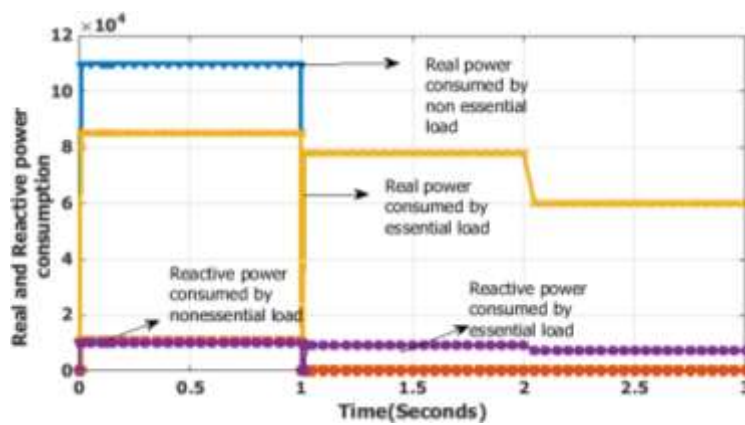


Figure 11. Real and reactive power consumption of essential and non-essential loads

Figure 12 shows the voltage and current waveforms of PV source connected at bus 1. Figure 13 showcase the voltage and current waveforms of backup modules connected at bus 1. Figure 12 witness a captivating interplay of power dynamics, where the PV panels, battery, and super capacitor engage in a delicate balancing act, their contributions fluidly fluctuating to meet the needs of both the grid and the loads they serve. The PMA stands as a vigilant protector of DG1's energy reserves, expertly guiding the battery and SC to safeguard power availability even when external sources falter or disappear. The essential load receives unwavering support from DG1, with its 80 kW demand met through a balanced combination of solar power, battery power, and supercapacitor power, ensuring that critical operations remain unimpeded.

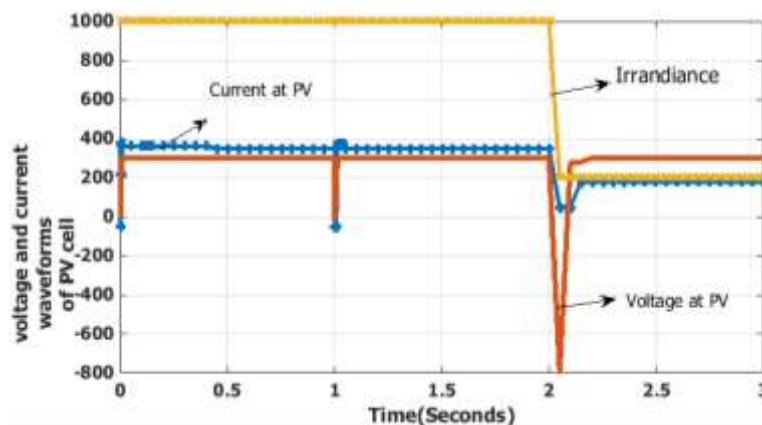


Figure 12. Voltage and current waveforms of PV connected at bus 1

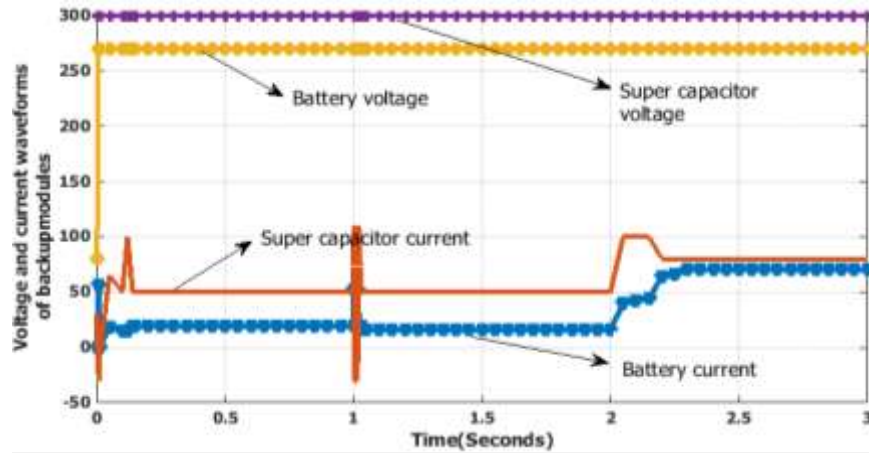


Figure 13. Voltage and current waveforms of backup modules connected at bus 1

The DG units connected at bus 3 and 4 fails to compensate for the local loads during islanding mode because they do not have backup support with PMA control. Figure 14 shows the waveforms of active power output at bus 1 with and without PMA. Figure 15 shows the waveforms of reactive power output at bus 1 with and without PMA. As shown in the graph, the DG1 unit is able to maintain active power injection even after the grid is disconnected when it is integrated with backup modules and power management algorithm. However, when the grid is connected, the DG1 unit does not inject any reactive power. During islanding mode, the DG1 unit compensates for the reactive power of the essential load.

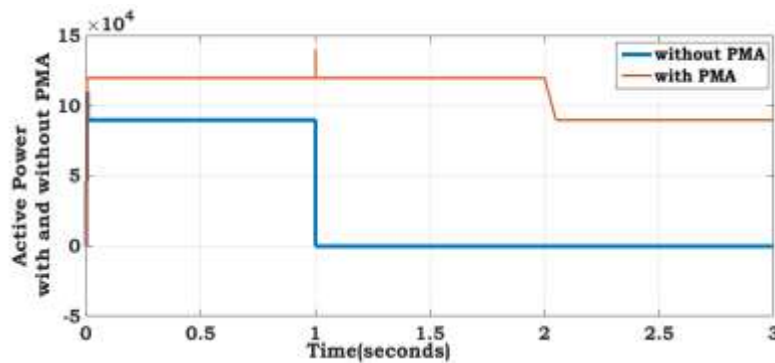


Figure 14. Active power output of test system connected at bus 1 with and without PMA

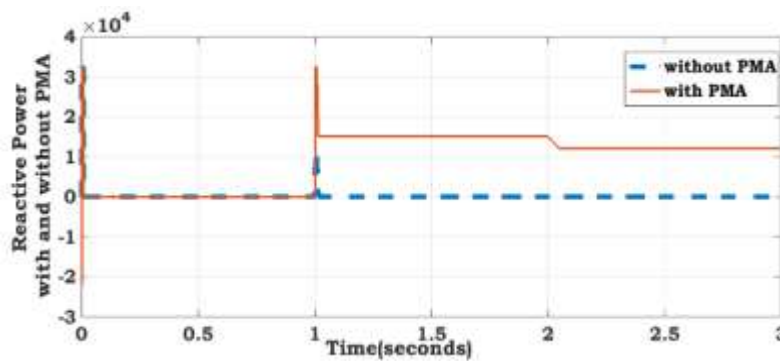


Figure 15. Reactive power output of test system connected at bus 1 with and without PMA

5. CONCLUSION

The test system has three renewable energy DG units connected at buses 1, 3 and 4. DG1 at bus 1 has backup storage sources to eliminate the drawbacks of islanding mode operation. The battery and SC modules support the PV source to compensate for the critical load. A high-gain DC-DC boost converter controlled with the dual Kalman filter-based perturb and observe method is used to attain maximum output power from the PV system. When the islanding detection algorithm identifies a grid disconnection, it removes the non-essential load from bus 1. A sliding mode current controller is designed to track the undisturbed reference voltage at the three-phase inverter with LC filter. To effectively manage the power flow and optimize the utilization of available resources, a robust power management algorithm control is used to ensure the reliable operation of a microgrid during islanding mode. The PMA control can dynamically allocate power among various sources, storage systems, and loads, considering their characteristics and the overall system constraints. The results from the simulation study show that the PMA control can enable the DG units to maintain active power injection even after the grid is disconnected. The PMA control can also compensate for the reactive power of the essential load during islanding mode. Overall, the PMA control is a promising solution for the reliable operation of microgrids with renewable energy sources and hybrid energy backup.





REFERENCES

- [1] A. Bharatee, P. K. Ray, B. Subudhi, and A. Ghosh, "Power management strategies in a hybrid energy storage system integrated AC/DC microgrid: a review," *Energies*, vol. 15, no. 19, p. 7176, Sep. 2022, doi: 10.3390/en15197176.
- [2] P. Annapandi, R. Banumathi, N. S. Pratheeba, and A. A. Manuela, "An efficient optimal power flow management based microgrid in hybrid renewable energy system using hybrid technique," *Transactions of the Institute of Measurement and Control*, vol. 43, no. 1, pp. 248–264, Oct. 2021, doi: 10.1177/0142331220961687.
- [3] U. B. Tayab, J. Lu, F. Yang, T. S. AlGarni, and M. Kashif, "Energy management system for microgrids using weighted salp swarm algorithm and hybrid forecasting approach," *Renewable Energy*, vol. 180, pp. 467–481, Dec. 2021, doi: 10.1016/j.renene.2021.08.070.
- [4] S. Jamal, N. M. L. Tan, and J. Pasupuleti, "A review of energy management and power management systems for microgrid and nanogrid applications," *Sustainability (Switzerland)*, vol. 13, no. 18, p. 10331, Sep. 2021, doi: 10.3390/su131810331.
- [5] Y. E. G. Vera, R. Dufo-López, and J. L. Bernal-Agustín, "Energy management in microgrids with renewable energy sources: A literature review," *Applied Sciences (Switzerland)*, vol. 9, no. 18, p. 3854, Sep. 2019, doi: 10.3390/app9183854.
- [6] H. Armghan, M. Yang, A. Armghan, N. Ali, M. Q. Wang, and I. Ahmad, "Design of integral terminal sliding mode controller for the hybrid AC/DC microgrids involving renewables and energy storage systems," *International Journal of Electrical Power and Energy Systems*, vol. 119, p. 105857, Jul. 2020, doi: 10.1016/j.ijepes.2020.105857.
- [7] R. Benadli, B. Khiari, M. Memmi, M. Bjaoui, and A. Sellami, "An improved super-twisting sliding mode control for standalone hybrid wind/photovoltaic/fuel cell system based on energy management of battery/hydrogen," *Journal of Solar Energy Engineering, Transactions of the ASME*, vol. 144, no. 3, Mar. 2022, doi: 10.1115/1.4053748.
- [8] Y. Yang and S. C. Tan, "Trends and development of sliding mode control applications for renewable energy systems," *Energies*, vol. 12, no. 15, p. 2861, Jul. 2019, doi: 10.3390/en12152861.
- [9] G. Nisha and K. Jamuna, "Real-time implementation of sliding mode controller for standalone microgrid systems for voltage and frequency stabilization," *Energy Reports*, vol. 10, pp. 768–792, Nov. 2023, doi: 10.1016/j.egy.2023.07.015.
- [10] R. G. Allwyn, A. Al-Hinai, and V. Margaret, "A comprehensive review on energy management strategy of microgrids," *Energy Reports*, vol. 9, pp. 5565–5591, Dec. 2023, doi: 10.1016/j.egy.2023.04.360.
- [11] M. Zolfaghari, M. Abedi, and G. B. Gharehpetian, "Power flow control of interconnected AC-DC microgrids in grid-connected hybrid microgrids using modified UIPC," *IEEE Transactions on Smart Grid*, vol. 10, no. 6, pp. 6298–6307, Nov. 2019, doi: 10.1109/TSG.2019.2901193.
- [12] Y. K. Semero, J. Zhang, and D. Zheng, "Optimal energy management strategy in microgrids with mixed energy resources and energy storage system," *IET Cyber-Physical Systems: Theory and Applications*, vol. 5, no. 1, pp. 80–84, Nov. 2020, doi: 10.1049/iet-cps.2019.0035.
- [13] J. Faria, J. Pombo, M. do Rosário Calado, and S. Mariano, "Power management control strategy based on artificial neural networks for standalone PV applications with a hybrid energy storage system," *Energies*, vol. 12, no. 5, p. 902, Mar. 2019, doi: 10.3390/en12050902.
- [14] N. Altin and S. E. Eyimaya, "A review of microgrid control strategies," in *10th IEEE International Conference on Renewable Energy Research and Applications, ICRERA 2021*, Sep. 2021, pp. 412–417, doi: 10.1109/ICRERA52334.2021.9598699.
- [15] I. Saady, M. Karim, B. Bossoufi, N. El Ouanjli, S. Motahhir, and B. Majout, "Optimization and control of photovoltaic water pumping system using kalman filter based MPPT and multilevel inverter fed DTC-IM," *Results in Engineering*, vol. 17, p. 100829, Mar. 2023, doi: 10.1016/j.rineng.2022.100829.
- [16] M. Russo and G. Fusco, "Robust decentralized PI controllers design for voltage regulation in distribution networks with DG," *Electric Power Systems Research*, vol. 172, pp. 129–139, Jul. 2019, doi: 10.1016/j.epsr.2019.01.039.
- [17] J. Li, Z. Xu, J. Zhao, and C. Zhang, "Distributed online voltage control in active distribution networks considering PV curtailment," *IEEE Transactions on Industrial Informatics*, vol. 15, no. 10, pp. 5519–5530, Oct. 2019, doi: 10.1109/TII.2019.2903888.
- [18] S. K. Bilgundi, H. Pradeepa, A. Kadam, and L. M. Venkatesh, "Energy management schemes for distributed energy resources connected to power grid," *Indonesian Journal of Electrical Engineering and Computer Science*, vol. 28, no. 1, pp. 30–40, Oct. 2022, doi: 10.11591/ijeecs.v28.i1.pp30-40.
- [19] G. Fusco and M. Russo, "Tuning of multivariable PI robust controllers for the decentralized voltage regulation in grid-connected distribution networks with Distributed Generation," *International Journal of Dynamics and Control*, vol. 8, no. 1, pp. 278–290, Mar. 2020, doi: 10.1007/s40435-019-00528-7.





- [20] M. Badoni, A. Singh, A. K. Singh, H. Saxena, and R. Kumar, "Grid tied solar PV system with power quality enhancement using adaptive generalized maximum versoria criterion," *CSEE Journal of Power and Energy Systems*, vol. 9, no. 2, pp. 722–732, 2023, doi: 10.17775/CSEEJPES.2020.04820.
- [21] N. Chaitanya, S. Yamparala, K. Radharani, and P. P. Prasanthi, "Optimized power management control scheme for transportation system electrified with high voltage DC microgrid," *International Journal of Renewable Energy Research*, vol. 12, no. 1, pp. 536–546, 2022, doi: 10.20508/ijrer.v12i1.12793.g8427.
- [22] X. Li *et al.*, "A robust autonomous sliding-mode control of renewable DC microgrids for decentralized power sharing considering large-signal stability," *Applied Energy*, vol. 339, p. 121019, Jun. 2023, doi: 10.1016/j.apenergy.2023.121019.
- [23] M. Uddin, H. Mo, D. Dong, S. Elsayah, J. Zhu, and J. M. Guerrero, "Microgrids: A review, outstanding issues and future trends," *Energy Strategy Reviews*, vol. 49, p. 101127, Sep. 2023, doi: 10.1016/j.esr.2023.101127.
- [24] A. J. Abianeh and F. Ferdowsi, "Sliding mode control enabled hybrid energy storage system for islanded DC microgrids with pulsing loads," *Sustainable Cities and Society*, vol. 73, p. 103117, Oct. 2021, doi: 10.1016/j.scs.2021.103117.
- [25] K. Rayane, M. Bougrine, A. Benalia, and K. Guesmi, "Sliding mode control of a three-phase inverter with an output LC filter," Nov. 2018, doi: 10.1109/ICASS.2018.8651964.

BIOGRAPHIES OF AUTHORS



Veeranjanyulu Gopu     is an Assistant professor in Electrical and Electronics Engineering Department at the RVR&JC College of Engineering, Guntur, India. He received his B.Tech. and M.Tech. degrees in Electrical and Electronics Engineering from Jawaharlal Nehru Technological university, Hyderabad and Acharya Nagarjuna University, Guntur, in 2007, and 2009, respectively. He has been an Assistant Professor in RVR&JC College of Engineering, Guntur, India since 2013. His research interests include the field of power systems, power electronics, motor drives, renewable energy and microgrid. He can be contacted at email: gvanjaneyulu@rvrjc.ac.in.



Dr. Mudakapla Shadaksharappa Nagaraj     is a Professor and Head of Department in Electrical & Electronic Engineering Department, BIET, Davangere since 2008. He completed his B.E (E & E) degree from Government BDT College of Engineering, Davangere, Mysore University in 1986 and perused his Master degree in Power systems from NIE, Mysore, Mysore University in 1990. He received his doctorate from Visvesvaraya Technological University during 2008. Presently, he is guiding 2 Ph.D. students and 5 research scholars are awarded with Ph.D. under VTU, Belagavi. He is Life Member of Indian Society for Technical Education and Member of Institution of Engineers (MIE). He has awarded as best teacher for several times from the college for achieving 100% result in various subjects handled. His research interests include the field of electrical load forecasting, reactive power compensation, economic scheduling, contingency analysis, control systems, power electronics, artificial neural network, fuzzy logic. He can be contacted at email:msndvg@gmail.com.